

Elastic scattering of positive muons from ^3He and ^4He M.-S. Wu^{1,2}, Y. Zhang^{1,2,*}, G.-A. Yan³, J.-Y. Zhang^{4,†}, K. Varga⁵ and Z.-C. Yan^{6,4}¹Center for Theoretical Physics, Hainan University, Haikou 570228, China²School of Science, Hainan University, Haikou 570228, China³School of Physics and Physical Engineering, Qufu Normal University, Qufu 273165, China⁴State Key Laboratory of Magnetic Resonance and Atomic and Molecular Physics, Innovation Academy for Precision Measurement Science and Technology, Chinese Academy of Sciences, Wuhan 430071, China⁵Department of Physics and Astronomy, Vanderbilt University, Nashville, Tennessee 37235, USA⁶Department of Physics, University of New Brunswick, Fredericton, New Brunswick, Canada E3B 5A3

(Received 21 March 2023; accepted 17 April 2023; published 25 April 2023)

The study of positive muon μ^+ -He scattering plays an important role in precision experiments involving positive muons. In this paper, we employed the confined variational method to investigate S -wave μ^+ -He scattering with scattering momenta below $0.1a_0^{-1}$, where a_0 denotes the Bohr radius. Our approach yielded accurate S -wave phase shifts and scattering lengths. By utilizing the modified effective range formula, we determined the S -wave scattering lengths to be $-12.3a_0$ and $-10.6a_0$ for μ^+ - ^4He and μ^+ - ^3He scattering, respectively. Furthermore, we examined the distortion effects on helium induced by μ^+ .

DOI: [10.1103/PhysRevA.107.042815](https://doi.org/10.1103/PhysRevA.107.042815)

I. INTRODUCTION

The positive muon μ^+ , which is the antiparticle of the muon, holds a special significance in testing the theory of quantum electrodynamics (QED) and searching for new physics beyond the standard model of elementary particle physics (BSM) [1–7]. One of the most notable examples is the Muon $g - 2$ experiment, which has provided stronger evidence for BSM physics [1]. Recently, Delaunay *et al.* [8] and Ohayon *et al.* [9] have proposed that muonium spectroscopy could serve as an alternative approach for determining the muon anomalous magnetic moment. To meet the requirements of these precision experiments, μ^+ needs to be trapped and cooled to low temperatures as standard μ^+ beams possess relatively high energy and poor phase space quality [10]. For instance, the muCool device has been developed at the Paul Scherrer Institute (PSI), which uses cryogenic helium buffer gas for precooling [11,12]. Hence, studying μ^+ -He scattering is essential for enhancing the cooling process in these muon precision experiments.

The process of slowing down μ^+ in low-pressure He gas has been studied by Fleming *et al.* [13] and Senba [14]. Fournier *et al.* [15] performed calculations of the binding energies of ^4He μ^+ using the Born-Oppenheimer (BO) potential of HeH^+ . Cencek *et al.* [16], Stanke *et al.* [17,18], Tung *et al.* [19], and Pachucki [20] further improved the BO potentials for HeH^+ and its isotopic combinations. Yang *et al.* [21] used explicitly correlated Gaussians (ECGs) to calculate the high-accuracy binding energies of all the bound states of ^4He μ^+ without applying the BO approximation. They confirmed that the BO approximation is reasonable for ^4He μ^+ , as it can be regarded as a system of a positive muon bound to a slightly

distorted helium atom. However, *ab initio* calculations still need to be performed for μ^+ -He scattering.

In this paper, we calculate the scattering properties of μ^+ - ^4He and μ^+ - ^3He using the confined variational method (CVM) combined with ECGs. The CVM is an *ab initio* method used for studying low-energy elastic scattering problems. It has been widely applied to investigate the scattering of electron, positron, and positronium with hydrogen, helium, and hydrogen molecular systems [22–27]. Very recently, a strategy was developed that can effectively eliminate the non-physical confinement effect of the original CVM [28,29]. In addition, unlike the original CVM, this strategy uses a smaller confining radius, which greatly reduces the computational cost.

This paper is organized as follows: In Sec. II, we introduce the CVM. We present the computational results in Sec. III, where we provide the phase shifts in Sec. III A, the S -wave scattering lengths in Sec. III B, and the distortions of the helium atoms during the scattering processes in Sec. III C. Finally, a summary is given in Sec. IV. Phase shifts are expressed in radians, and atomic units (a.u.) are used throughout unless otherwise stated.

II. THEORY

The scattering of μ^+ -He, in the absence of the BO approximation, represents a fundamental four-body Coulomb problem. The Hamiltonian of the system, in the laboratory frame, is given by

$$\mathcal{H} = \sum_{i=1}^4 \frac{\mathbf{p}_i^2}{2m_i} + \sum_{\substack{i,j=1 \\ j>i}}^4 \frac{q_i q_j}{|\mathbf{r}_i - \mathbf{r}_j|}, \quad (1)$$

where \mathbf{r}_i , m_i , and q_i denote the position vector, mass, and charge of the i th particle, respectively, and \mathbf{p}_i is the

*yzhang@hainanu.edu.cn

†jzhang@apm.ac.cn

momentum conjugate to \mathbf{r}_i . In particular, particle 1 refers to the helium nucleus, particles 2 and 3 represent the two electrons, and the last particle 4 corresponds to the positive muon.

After removing the center-of-mass motion from \mathcal{H} and setting the helium nucleus as the origin of the coordinate system, the internal Hamiltonian of the scattering system takes the form

$$H = \frac{1}{2} \sum_{i,j=1}^3 \Lambda_{ij} \pi_i \cdot \pi_j + \sum_{i=1}^3 \frac{q_1 q_{i+1}}{|\mathbf{x}_i|} + \sum_{\substack{i,j=1 \\ j>i}}^3 \frac{q_{i+1} q_{j+1}}{|\mathbf{x}_i - \mathbf{x}_j|}, \quad (2)$$

where $\mathbf{x}_i = \mathbf{r}_{i+1} - \mathbf{r}_1$ are the internal relative coordinates and $\pi_i = -i\partial/\partial\mathbf{x}_i$ are the momenta conjugate to \mathbf{x}_i . Also, $\Lambda_{ij} = \sum_{k=1}^4 U_{ik} U_{jk} / m_k$ ($i, j = 1, 2, 3$), with the transformation matrix U defined by

$$U = \begin{pmatrix} -1 & 1 & 0 & 0 \\ -1 & 0 & 1 & 0 \\ -1 & 0 & 0 & 1 \\ \frac{m_1}{m_i} & \frac{m_2}{m_i} & \frac{m_3}{m_i} & \frac{m_4}{m_i} \end{pmatrix}, \quad (3)$$

where $m_i = \sum_{j=1}^4 m_j$ is the total mass of the system.

The CVM approach involves the use of a confining potential V_{cp} to transform the original many-body scattering problem into a confined many-body bound-state problem. According to CVM, when two potentials V_1 and V_2 have the same eigenenergy E under the same confining potential V_{cp} , they will exhibit the same phase shift at energy E [22,26]. Suppose V_1 represents the actual potential between a μ^+ particle and helium, and V_2 is an unknown, adjustable potential. The CVM can help us construct this auxiliary potential V_2 and then solve the scattering equation of V_2 to obtain the phase shift of the original μ^+ -He scattering problem.

The specific procedures to determine V_2 are as follows. Initially, a many-body calculation is carried out by incorporating a confining potential V_{cp} into the internal Hamiltonian of the original μ^+ -He scattering problem,

$$(H + V_{\text{cp}})\Psi(\mathbf{x}, \mathbf{s}) = E\Psi(\mathbf{x}, \mathbf{s}), \quad (4)$$

where \mathbf{x} refers to $(\mathbf{x}_1, \mathbf{x}_2, \mathbf{x}_3)$ and \mathbf{s} refers to $(\mathbf{s}_1, \mathbf{s}_2, \mathbf{s}_3, \mathbf{s}_4)$, representing the spins of the four particles. The function Ψ is the eigenfunction of $H + V_{\text{cp}}$ that corresponds to the eigenenergy E . The eigenenergy E is the sum of the ground-state energy of He and the scattering energy $E_s = k^2/(2m_r)$, with k being the scattering momentum and m_r the reduced mass between μ^+ and He. In order to account for the intricate Coulomb correlations between particles, the many-body wave function Ψ is expanded in terms of the explicitly correlated Gaussians (ECGs) [30–32],

$$\Psi = \sum_{n=1}^N c_n \phi_n, \quad (5)$$

$$\phi_n = |\mathbf{v}|^{2K_n+L} \exp\left(-\frac{1}{2} \mathbf{x}^T A_n \mathbf{x}\right) Y_{LM}(\mathbf{v}) \chi(\mathbf{s}), \quad (6)$$

where N is the basis size and c_n are the expansion coefficients. Furthermore, \mathbf{v} represents the global vector [30], $\chi(\mathbf{s})$ represents the spin function, A_n is a parameter matrix, K_n is

an integer, and $|\mathbf{v}|^{2K_n}$ is an important factor that describes the wave function between μ^+ and He. Lastly, L and M are, respectively, the total orbital angular momentum and its z component, while Y_{LM} denotes the spherical harmonics.

The potential used in this study [22,26] is given by

$$V_{\text{cp}}(\rho) = \begin{cases} 0, & \rho < R_0, \\ G(\rho - R_0)^2, & \rho \geq R_0, \end{cases} \quad (7)$$

where ρ represents the distance between the center of mass of helium and μ^+ , and R_0 is the confining radius. The value of R_0 is chosen such that the complex short-range interaction between μ^+ and helium can be neglected outside the sphere of radius R_0 . In this study, we set R_0 equal to 18.

The confining potential in Eq. (4), or equivalently the parameter G in Eq. (7), is adjusted to produce a specific total eigenenergy E . Once the confining potential $V_{\text{cp}}(\rho)$ is determined for this specific E , we can proceed to solve the one-dimensional bound-state problem:

$$\left(-\frac{1}{2m_r} \frac{d^2}{d\rho^2} + V_2(\rho) + V_{\text{cp}}(\rho)\right)\Phi(\rho) = E'\Phi(\rho). \quad (8)$$

In this step, we aim to determine an adjustable model potential V_2 that produces the same scattering energy E_s under the same confining potential V_{cp} . Here, $\Phi(\rho)$ and E' represent, respectively, the eigenfunction and the associated eigenvalue. We choose $V_2(\rho)$ to be

$$V_2(\rho) = \lambda e^{-\alpha\rho} - \frac{\alpha_d}{2\rho^4} [1 - e^{-(\rho/\beta)^6}], \quad (9)$$

where λ , α , and β are adjustable parameters. The term $-\alpha_d/(2\rho^4)$ is the long-range polarization potential, with $\alpha_d = 1.383\,200$ being the ground-state polarizability of helium [33]. In this work, we set $\alpha = 0.5$ and $\beta = 5$, and adjust λ to ensure that the bound-state problem Eq. (8) yields the eigenvalue $E' = E_s = k^2/(2m_r)$ for given k . Once we have determined the parameter λ from Eq. (8), we can determine the phase shift of μ^+ -He scattering by solving the one-dimensional scattering equation for V_2 :

$$\left(-\frac{1}{2m_r} \frac{d^2}{d\rho^2} + V_2(\rho)\right)\phi(\rho) = E_s \phi(\rho). \quad (10)$$

It is worth noting that the calculated CVM phase shifts are independent of the form of V_2 . This is due to the fact that the phase shift is determined solely by the logarithmic derivative of the wave function, and the derivatives at each step have been shown to be equal [22,23,27].

III. RESULTS

A. Phase shifts

In this study, we use masses of 7294.299 541 42 for the ${}^4\text{He}$ nucleus, 5495.885 280 07 for the ${}^3\text{He}$ nucleus, and 206.768 283 0 for μ^+ [34]. The ground-state energies of atomic ${}^4\text{He}$ and ${}^3\text{He}$ are calculated to be $E_{\text{He}} = -2.903\,304\,557$ and $E_{\text{He}} = -2.903\,167\,210$, respectively, using 700 ECGs.

Table I presents the convergence test results of the many-body eigenvalue E , the model potential parameter λ , and the S -wave phase shift δ for μ^+ - ${}^4\text{He}$ scattering at $k = 0.1$,

TABLE I. Convergence test for the many-body eigenvalue E in Eq. (4), the model potential parameter λ in Eq. (9), and the S -wave phase shift δ (in radians) at $k = 0.1$ for μ^+ - ^4He scattering, as the size of the basis set N increases. In atomic units.

N	E	λ	δ
3100	-2.903 279 660	0.009 262 029	0.046 82
3400	-2.903 279 672	0.009 257 924	0.047 60
3700	-2.903 279 679	0.009 255 532	0.048 06
4000	-2.903 279 684	0.009 253 824	0.048 38

as the basis set size N increases. It is noted that the exact corresponding many-body eigenvalue in Eq. (4) is $E = E_{\text{He}} + (0.1)^2/(2m_r) = -2.903\,279\,690$. We observe that E , λ , and δ converge smoothly to the eighth, third, and second significant digit, respectively. Therefore, in this work, we use $N = 4000$ for all calculations of the S -wave phase shifts of μ^+ - ^4He and μ^+ - ^3He scatterings.

As the mass of μ^+ is significant compared to that of a helium nucleus, it is necessary to use finite helium nuclear mass when studying μ^+ -He scattering. In contrast, for e^+ -He scattering, the infinite nuclear mass approximation can be used. In a test run, for example, with only 2000 ECGs, the S -wave phase shift for e^+ -He scattering at $k = 0.1$ has already converged to the third significant digit.

The difference between the CVM calculations for μ^+ -He scattering and e^+ -He scattering can be explained as follows. For e^+ -He scattering with $L = 0$, there is no bound state between the positron and helium, so the first bound state in Eq. (4) is optimized in our CVM calculation. However, for μ^+ -He scattering with $L = 0$, there are four bound states between μ^+ and helium, so the fifth bound state in Eq. (4) is optimized. In other words, the CVM calculation of μ^+ -He scattering is more difficult than that of e^+ -He scattering, and as a result, more ECGs are required, and fewer significant digits are expected to converge.

Due to the level of difficulties of calculating μ^+ -He scattering using CVM, only S -wave scattering was studied in this work. Table II displays the S -wave phase shifts for μ^+ - ^4He and μ^+ - ^3He scattering at $k = 0.06$ – 0.1 . All phase shifts in this table are accurate to the second significant digit. Due

TABLE II. S -wave phase shifts (in radians) obtained by the confined variational method for μ^+ - ^4He and μ^+ - ^3He scattering at $k = 0.06 - 0.1$, and by the Born-Oppenheimer (BO) potential of HeH^+ . In atomic units.

	k	δ	$\delta(\text{BO})$
μ^+ - ^4He	0.06	0.32	0.38
	0.07	0.25	0.31
	0.08	0.19	0.23
	0.09	0.12	0.16
	0.1	0.048	0.088
μ^+ - ^3He	0.06	0.26	0.31
	0.07	0.20	0.25
	0.08	0.13	0.18
	0.09	0.066	0.10
	0.1	-0.0044	0.032

TABLE III. S -wave scattering lengths a_s for μ^+ - ^4He , μ^+ - ^3He , and e^+ -He scattering using the confined variational method (CVM), the Born-Oppenheimer (BO) potential of HeH^+ , and the stochastic variational method (SVM). In atomic units.

System	Method	a_s
μ^+ - ^4He	CVM	-12.3
	BO	-14.0
μ^+ - ^3He	CVM	-10.6
	BO	-11.9
e^+ -He	SVM	-0.474

to the difference in mass between ^4He and ^3He , their phase shifts are noticeably distinct. As k decreases, the percentage differences in the phase shifts between μ^+ - ^4He and μ^+ - ^3He scattering decrease. For each scattering, the phase shifts decrease as k increases, which is the opposite of those in e^+ -He scattering. The S -wave phase shift of e^+ -He scattering at $k = 0.1$ is 0.03 [35,36], which is similar to that of μ^+ - ^4He scattering. Moreover, the convergence of the phase shifts of μ^+ - ^3He scattering is slower than that of μ^+ - ^4He scattering, indicating that the former is more difficult to calculate using CVM. The phase shift of μ^+ - ^3He scattering changes sign from positive at $k = 0.09$ to negative at $k = 0.1$, while for μ^+ - ^4He scattering it does not, suggesting that the S -wave interaction is more attractive for μ^+ - ^4He scattering than for μ^+ - ^3He scattering at the same k . For comparison, Table II also lists the S -wave phase shifts obtained by the Born-Oppenheimer (BO) potential of HeH^+ [20] using a five-point polynomial interpolation. These BO phase shifts are more positive than our CVM results, indicating that the BO potential is more attractive for μ^+ -He scattering.

B. Scattering length

The S -wave scattering length is a crucial parameter in experiments involving cold or ultracold atoms and molecules. However, currently, experimental or theoretical results for the S -wave scattering length of μ^+ -He scattering are lacking. In this study, we obtain the S -wave scattering lengths by fitting the calculated phase shifts to the well-known effective range expansion given by

$$k \cot \delta_k = -\frac{1}{a_s} + \frac{r_e k^2}{2}, \quad (11)$$

where δ_k is the phase shift corresponding to the momentum k , a_s is the S -wave scattering length, and r_e is the effective range. In order to take into account the long-range polarization potential $-\alpha_d/(2\rho^4)$, we use the modified effective range expansion [37],

$$\tan \delta_k = -a_s k \left(1 + \frac{4\alpha_d k^2}{3} \ln k \right) - \frac{\pi \alpha_d k^2}{3} + Dk^3 + Fk^4, \quad (12)$$

where D and F are two additional fitting parameters. It is noted that higher-order terms ignored in these formulas do not significantly impact low- k scattering processes.

The results of the scattering lengths obtained by the CVM, as determined by Eq. (12), are presented in Table III.

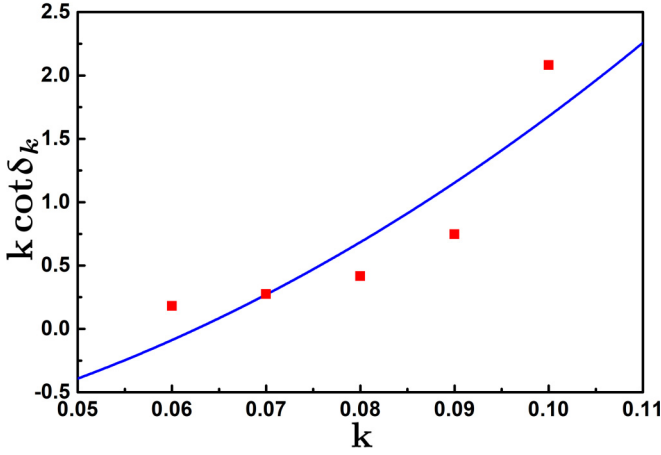


FIG. 1. The fitting result between the calculated S -wave phase shifts (in radians) from the CVM and the effective range expansion Eq. (11) for μ^+ - ^4He scattering at $k = 0.06$ – 0.1 . In atomic units.

A comparison with the results calculated by the Born-Oppenheimer (BO) potential of HeH^+ [20] is provided. Additionally, the scattering length of e^+ -He scattering, obtained by the stochastic variational method (SVM) under the infinite nuclear mass approximation [38], is also included.

Note that the CVM and BO scattering lengths are extracted from the phase shifts in Table II. The fitting results for the CVM phase shifts of μ^+ - ^4He scattering using Eqs. (11) and (12) are shown in Figs. 1 and 2, respectively. From the two figures, it is clear that the correct result cannot be obtained using Eq. (11), while Eq. (12) fits well with the calculated data. This indicates that the long-range polarization potential has a significant influence on the μ^+ -He scattering length.

The CVM scattering lengths of μ^+ - ^4He and μ^+ - ^3He , determined by Eq. (12), are -12.3 and -10.6 , respectively. The percentage differences between the CVM scattering lengths and the BO results are 14% and 12% for μ^+ - ^4He and μ^+ - ^3He , respectively.

The scattering length of e^+ -He is -0.474 , which is less negative compared to the scattering lengths of μ^+ -He. This suggests that the interaction between μ^+ and He is more

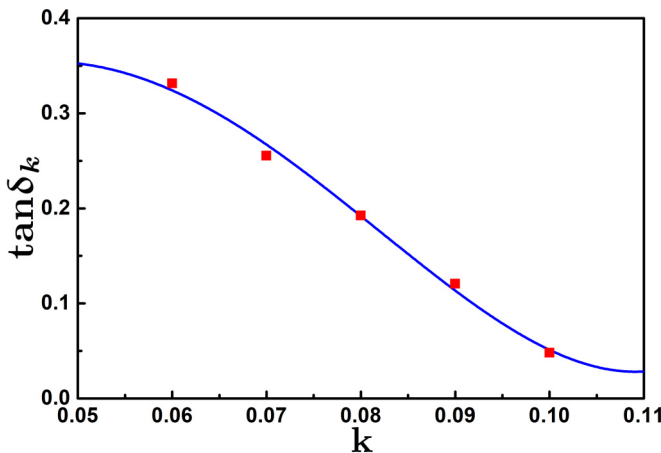


FIG. 2. The fitting result between the calculated S -wave phase shifts (in radians) from the CVM and the effective range expansion Eq. (12) for μ^+ - ^4He scattering at $k = 0.06$ – 0.1 . In atomic units.

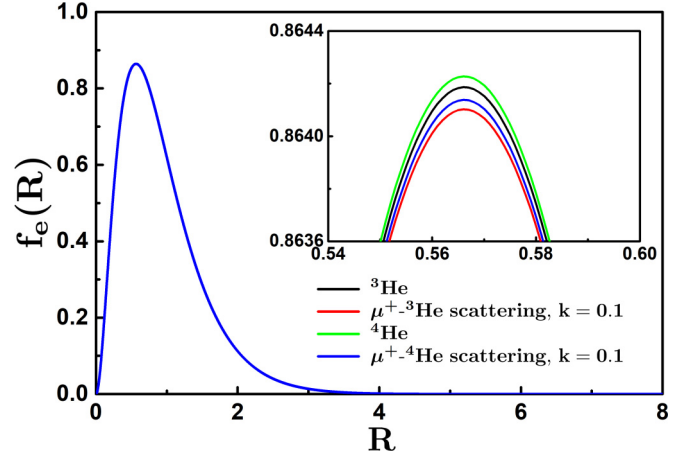


FIG. 3. Probability density functions for the ground states of ^4He and ^3He , as well as the μ^+ - ^4He and μ^+ - ^3He scatterings at $k = 0.1$. In atomic units.

attractive at low energies. Although μ^+ has the same charge as e^+ , the larger mass of μ^+ greatly reduces the value of the kinetic energy, resulting in a more attractive interaction with helium.

C. Distortion effects

When a helium atom and μ^+ come into close proximity, the helium atom undergoes distortion. In a previous study by Yang *et al.* [21], it was confirmed that the bound state of ^4He μ^+ can be considered as a system where a μ^+ is bound to a slightly distorted helium atom. However, the effects of distortion in the μ^+ - ^3He and μ^+ - ^4He scatterings, and their comparison, still need to be studied.

To provide a quantitative analysis of helium atom distortion, we use the probability density function of the electron $f_e(R)$,

$$f_e(R) = R^2 \int d\Omega_R \langle \Psi | \frac{\delta(\mathbf{x}_1 - \mathbf{R}) + \delta(\mathbf{x}_2 - \mathbf{R})}{2} | \Psi \rangle, \quad (13)$$

where the symbol $\langle \dots \rangle$ indicates integration over the two electron coordinates \mathbf{x}_1 and \mathbf{x}_2 relative to the helium nucleus, while $\int d\Omega_R \dots$ represents integration over the solid angle of vector \mathbf{R} .

Figure 3 shows the probability density function $f_e(R)$ for μ^+ - ^4He and μ^+ - ^3He scatterings at $k = 0.1$. For comparison, $f_e(R)$ of the ground-state ^3He and ^4He atoms are also included. The four $f_e(R)$ are quite similar, with a peak near $R = 0.566$. However, the peaks of μ^+ - ^3He and μ^+ - ^4He scatterings are lower than those of ^3He and ^4He , indicating that the distortion of helium in μ^+ - ^3He and μ^+ - ^4He scatterings is slightly greater. This is because $\int f_e(R) dR = 1$ holds for all four $f_e(R)$. The peak of μ^+ - ^3He is 0.0098% lower than that of ^3He , and the peak of μ^+ - ^4He is 0.0104% lower than that of ^4He , indicating that the helium distortions in μ^+ - ^3He and μ^+ - ^4He are very similar to each other.

Figure 4 displays the probability density function $f_e(R)$ for the ground state of the ^3He atom, the μ^+ - ^3He scattering at $k = 0.1$, and the first and fourth bound states of ^3He μ^+ . Notably, all four density functions exhibit a peak near $R = 0.566$. Comparing $f_e(R)$ of μ^+ - ^3He and ^3He , we can observe

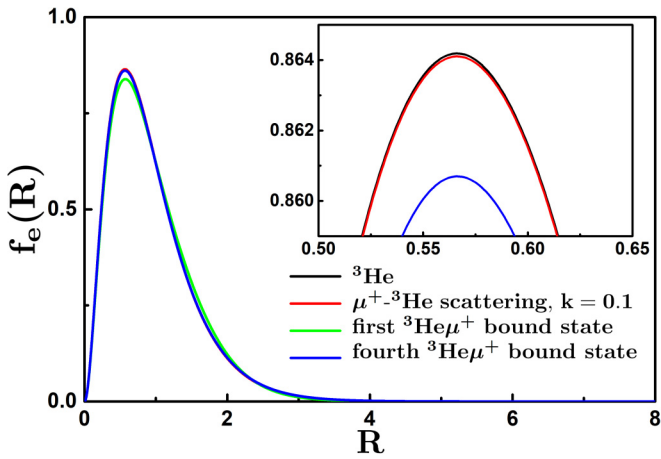


FIG. 4. Probability density functions for the ground state of ${}^3\text{He}$, the $\mu^+ - {}^3\text{He}$ scattering at $k = 0.1$, the first bound state of ${}^3\text{He} \mu^+$, and the fourth bound state of ${}^3\text{He} \mu^+$. In atomic units.

their similarity, but their peaks are evidently higher than those of the ${}^3\text{He} \mu^+$ bound states. This suggests that the helium distortion in the ${}^3\text{He} \mu^+$ bound states is greater. Additionally, the peak of the fourth ${}^3\text{He} \mu^+$ bound state is higher than that of the first bound state (which is not visible in the inset), implying that a larger helium distortion corresponds to a lower bound state. This is because as the positive muon approaches the helium atom, the distortion in the helium atom increases.

IV. SUMMARY

The confined variational method, in combination with an explicitly correlated Gaussian basis, was used to calculate the S -wave phase shifts and scattering lengths for low-energy elastic $\mu^+ - {}^4\text{He}$ and $\mu^+ - {}^3\text{He}$ scatterings without relying on the BO approximation. The S -wave phase shifts obtained through this method are converged to the second significant digit. By accounting for the long-range polarization effect, the S -wave scattering length was determined to be $-12.3a_0$ and $-10.6a_0$ for $\mu^+ - {}^4\text{He}$ and $\mu^+ - {}^3\text{He}$ scattering, respectively. Furthermore, the distortion of helium in $\mu^+ - {}^3\text{He}$ scattering was examined and compared to that of ${}^3\text{He} \mu^+$ bound states. The distortions in $\mu^+ - {}^3\text{He}$ scattering were found to be minimal, with the first ${}^3\text{He} \mu^+$ bound state exhibiting the largest distortion due to the proximity between μ^+ and ${}^3\text{He}$.

ACKNOWLEDGMENTS

This work was supported by the National Natural Science Foundation of China under Grants No. 12274106 and No. 12174399, by the Strategic Priority Research Program of the Chinese Academy of Sciences under Grant No. XDB21030300, and by the National Key Research and Development Program of China under Grant No. 2017YFA0304402. M.S.W. was supported by Hainan Provincial Natural Science Foundation of China under Grant No. 122MS005. Z.C.Y. was supported by the NSERC of Canada.

- [1] B. Abi (Muon $g - 2$ Collaboration), *Phys. Rev. Lett.* **126**, 141801 (2021).
- [2] S. Borsanyi, Z. Fodor, C. Hoelbling, T. Kawanai, S. Krieg, L. Lellouch, R. Malak, K. Miura, K. K. Szabo, C. Torrero, and B. C. Toth (Budapest-Marseille-Wuppertal Collaboration), *Phys. Rev. Lett.* **121**, 022002 (2018).
- [3] T. Blum, P. A. Boyle, V. Gülpers, T. Izubuchi, L. Jin, C. Jung, A. Jüttner, C. Lehner, A. Portelli, and J. T. Tsang (RBC and UKQCD Collaborations), *Phys. Rev. Lett.* **121**, 022003 (2018).
- [4] S. G. Karshenboim, *Phys. Rep.* **422**, 1 (2005).
- [5] P. Crivelli, *Hyperfine Interact.* **239**, 49 (2018).
- [6] S. G. Karshenboim, D. McKeen, and M. Pospelov, *Phys. Rev. D* **90**, 073004 (2014).
- [7] C. Frugiuele, J. Pérez-Ríos, and C. Peset, *Phys. Rev. D* **100**, 015010 (2019).
- [8] C. Delaunay, B. Ohayon, and Y. Soreq, *Phys. Rev. Lett.* **127**, 251801 (2021).
- [9] B. Ohayon, G. Janka, I. Cortinovis, Z. Burkley, L. de Sousa Borges, E. Depero, A. Golovizin, X. Ni, Z. Salman, A. Suter, C. Vigo, T. Prokscha, and P. Crivelli (Mu-MASS Collaboration), *Phys. Rev. Lett.* **128**, 011802 (2022).
- [10] D. Taqqu, *Phys. Rev. Lett.* **97**, 194801 (2006).
- [11] Y. Bao, A. Antognini, W. Bertl, M. Hildebrandt, K. S. Khaw, K. Kirch, A. Papa, C. Petitjean, F. M. Piegsa, S. Ritt, K. Sedlak, A. Stoykov, and D. Taqqu, *Phys. Rev. Lett.* **112**, 224801 (2014).
- [12] I. Belosevic, A. Antognini, Y. Bao, A. Eggenberger, M. Hildebrandt, R. Iwai, D. M. Kaplan, K. S. Khaw, K. Kirch, A. Knecht, A. Papa, C. Petitjean, T. J. Phillips, F. M. Piegsa, N. Ritjoho, A. Stoykov, D. Taqqu, and G. Wichmann, *Hyperfine Interact.* **240**, 41 (2019).
- [13] D. G. Fleming, R. J. Mikula, and D. M. Garner, *Hyperfine Interact.* **8**, 307 (1981).
- [14] M. Senba, *J. Phys. B: At., Mol. Opt. Phys.* **21**, 3093 (1988).
- [15] P. G. Fournier and R. J. Le Roy, *Chem. Phys. Lett.* **110**, 487 (1984).
- [16] W. Cencek, J. Komasa, and J. Rychlewski, *Chem. Phys. Lett.* **246**, 417 (1995).
- [17] M. Stanke, D. Kedziera, M. Molski, S. Bubin, M. Barysz, and L. Adamowicz, *Phys. Rev. Lett.* **96**, 233002 (2006).
- [18] M. Stanke, D. Kedziera, S. Bubin, and L. Adamowicz, *Phys. Rev. A* **77**, 022506 (2008).
- [19] W.-C. Tung, M. Pavanello, and L. Adamowicz, *J. Chem. Phys.* **137**, 164305 (2012).
- [20] K. Pachucki, *Phys. Rev. A* **85**, 042511 (2012).
- [21] H. Yang, M.-S. Wu, Y. Zhang, T.-Y. Shi, K. Varga, and J.-Y. Zhang, *Chin. Phys. B* **29**, 043102 (2020).
- [22] J. Mitroy, J. Y. Zhang, and K. Varga, *Phys. Rev. Lett.* **101**, 123201 (2008).
- [23] J. Y. Zhang, J. Mitroy, and K. Varga, *Phys. Rev. A* **78**, 042705 (2008).
- [24] J.-Y. Zhang, Z.-C. Yan, and U. Schwingenschlögl, *Europhys. Lett.* **99**, 43001 (2012).
- [25] J.-Y. Zhang, M.-S. Wu, Y. Qian, X. Gao, Y.-J. Yang, K. Varga, Z.-C. Yan, and U. Schwingenschlögl, *Phys. Rev. A* **100**, 032701 (2019).
- [26] J.-Y. Wan, M.-S. Wu, J.-Y. Zhang, and Z.-C. Yan, *Phys. Rev. A* **103**, 042814 (2021).
- [27] W. Du, M.-S. Wu, J.-Y. Zhang, Y. Qian, K. Varga, and Z.-C. Yan, *Phys. Rev. A* **105**, 052809 (2022).

- [28] M.-S. Wu, J.-Y. Zhang, X. Gao, Y. Qian, H.-H. Xie, K. Varga, Z.-C. Yan, and U. Schwingenschlögl, *Phys. Rev. A* **101**, 042705 (2020).
- [29] M.-S. Wu, J.-Y. Zhang, Y. Qian, K. Varga, U. Schwingenschlögl, and Z.-C. Yan, *Phys. Rev. A* **103**, 022817 (2021).
- [30] J. Mitroy, S. Bubin, W. Horiuchi, Y. Suzuki, L. Adamowicz, W. Cencek, K. Szalewicz, J. Komasa, D. Blume, and K. Varga, *Rev. Mod. Phys.* **85**, 693 (2013).
- [31] S. Bubin, M. Pavanello, W.-C. Tung, K. L. Sharkey, and L. Adamowicz, *Chem. Rev.* **113**, 36 (2013).
- [32] K. Varga and Y. Suzuki, *Phys. Rev. A* **53**, 1907 (1996).
- [33] Z.-C. Yan, J. F. Babb, A. Dalgarno, and G. W. F. Drake, *Phys. Rev. A* **54**, 2824 (1996).
- [34] E. Tiesinga, P. J. Mohr, D. B. Newell, and B. N. Taylor, *Rev. Mod. Phys.* **93**, 025010 (2021).
- [35] P. V. Reeth and J. W. Humberston, *J. Phys. B: At., Mol. Opt. Phys.* **32**, 3651 (1999).
- [36] D. G. Green, J. A. Ludlow, and G. F. Gribakin, *Phys. Rev. A* **90**, 032712 (2014).
- [37] M. R. Flannery, in *Springer Handbook of Atomic, Molecular, and Optical Physics*, edited by G. W. F. Drake (Springer, New York, 2006), 2nd ed., p. 668.
- [38] J. Y. Zhang and J. Mitroy, *Phys. Rev. A* **78**, 012703 (2008).